GEOPHYSICAL RESEARCH LETTERS, VOL. 28, NO. 17, PAGES 3389-3392, SEPTEMBER 1, 2001

Sediment effect on tsunami generation of the 1896 Sanriku tsunami earthquake

Yuichiro Tanioka

Seismology and Volcanology Research Department, Meteorological Research Institute, Tsukuba 305-0052, Japan

Tetsuzo Seno

Earthquake Research Institute, University of Tokyo, Tokyo 113-0032, Japan

Abstract. The 1896 Sanriku earthquake was one of the most devastating tsunami earthquakes, which generated an anomalously larger tsunami than expected from its seismic waves. Previous studies indicate that the earthquake occurred beneath the accretionary wedge near the trench axis. It was pointed out recently that sediments near a toe of an inner trench slope with a large horizontal movement due to the earthquake might have caused an additional uplift. In this paper, the effect of the additional uplift to tsunami generation of the 1896 Sanriku tsunami earthquake is quantified. We estimate the slip of the earthquake by numerically computing tsunamis and comparing their waveforms with those recorded at three tide gauges. The estimated slip for the model without the additional uplift is 10.4 m, and those with the additional uplift are 5.9-6.7 m. This indicates that the additional uplift of the sediments near the trench has a large effect on the tsunami generation.

1. Introduction

Most large, shallow earthquakes in subduction zones are tsunamigenic. Among them, unusual earthquakes that generate much larger tsunamis than expected from their seismic waves are called "tsunami earthquakes" [*Kanamori*, 1972]. The 1896 Sanriku tsunami earthquake that occurred along the Japan trench was one of the most anomalous earthquakes; the ground shaking was relatively weak, but the following tsunamis were devastating. *Abe* [1994] assigned the surface wave magnitude as M_s=7.2. The tsunami magnitude was determined as 8.6 from global data [*Abe*, 1979] and 8.2 from local data [*Abe*, 1981]. Recently, *Tanioka and Satake* [1996b] determined the fault parameters using the tsunami waveforms and estimated the moment magnitude as 8.0. The large discrepancy between Ms and Mt categorizes this event as a tsunami earthquake.

Satake and Tanioka [1999] showed that most moment release of tsunami earthquakes, including the 1896 Sanriku event, occurs in a narrow region near the trench. In this region, a large amount of unconsolidated or semiconsolidated sediments exist. The low angle thrust faulting near the trench on the decollement causes large horizontal movement perpendicular to the trench axis. *Seno* [2000] inferred from abnormal uplift associated with the horizontal movement of the 1999 Chi-Chi earthquake in Taiwan that sediments with horizontal movement on the decollement might have caused a large additional uplift. The horizontal trench-ward displacement of the backstop leads to overall folding of the accretionary prism. In this paper, we try to answer a key question: whether or not such an additional uplift near the trench causes a large tsunami? We compute the tsunami from the 1896 Sanriku event for ocean bottom deformation including elastic deformation due to faulting and the additional sediment uplift. Then, the effect of the additional uplift on the tsunami generation is discussed.

Paper number 2001GL013149.
0094-8276/01/2001GL013149$05.00

2. Three Models for Additional Uplift

The mechanism of the additional uplift is represented by the horizontal movement of the backstop scraping the sediments in front of it [*Seno*, 2000] as shown in Figure 1. This mechanism was originally suggested for the formation of the accretionary prism [*Davis et al.*, 1983; *Byrne et al.*, 1988], although the time scale is much longer than considered here for tsunami generation. We use three simplified models, Models A, B, and C, shown in Figure 2. In Model A, horizontal movement of the backstop uplifts sediments only above the slope of the backstop. In this model, the uplift of the sediments, u_s, is represented by $u_s=u_h\tan\theta$ where u_h is the horizontal movement due to the earthquake, and θ is the dip angle of the slope. *Tanioka and Satake* [1996a] used the same model to uplift water by the horizontal movement of a slope. In Model B, horizontal movement of the slope causes the uniform uplift of the whole sediments pile. In this model, with the mass balance, the uplift of the sediments, u_s, is represented by $u_s=u_hH/W$ where H is the height of the backstop slope, W is the width of the sediments, and u_h is the same as in Model A. Model A produces larger uplift in a narrower area, while Model B produces a smaller uplift in a wider area. These models are the two end members. In Model C, we assume that the sediment block behaves like rubber with an effective Poisson's ratio of 0.49. The surface deformation is computed

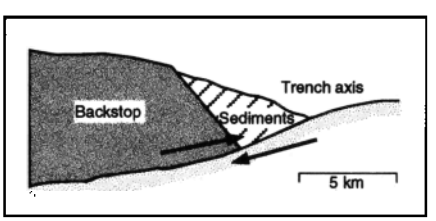

Figure 1. A schematic cross-section of the lower trench slope and trench wedge seen in the Japan Trench.

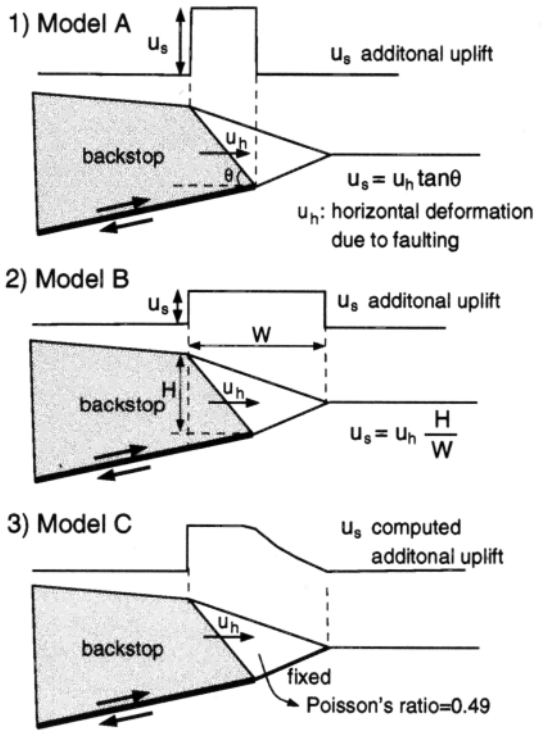

Figure 2. Three models for additional uplifts caused by sediments with horizontal movement of the backstop.

using the structural analysis software, MSC/NASTRAN, in which a finite element method is used. In this model, the bottom of the sediment block is fixed and the horizontal movement of the slope, u_h, due to the faulting is applied along the slope of the backstop.

In and around the northern part of the source region of the 1896 Sanriku earthquake, a detailed survey combining Seabeam mapping, single-channel seismic reflection observations, and gravity and geomagnetic measurements was conducted during Leg 3 of the French-Japanese KAIKO project [*Cadet et al.*, 1987]. The result of the mapping shows that there is a linear escarpment about 7 km landward of the trench axis and parallel to the axis. *Cadet et al.* [1987] indicates that, in front of the escarpment, there is a thick pile of sub-horizontal short reflections which represent reworked slump debris. From the reprocessed multichannel seismic record shown by *Cadet at al.* [1987], the height of the backstop (H) can be as large as 4 km and the dip angle of the scarp is about 50° (Figure 1). The sea beam survey by Hakuho-maru cruise KH90-1 [*Kobayashi et al.*, 1991] shows that the escarpment continues throughout the source region of the 1896 Sanriku earthquake and the average distance of the escarpment from the trench axis is about 7 km. Therefore, we assume that the width of the slump sediments is 7 km, the height of the backstop slope is 4 km, and the dip angle of the slope is 50° throughout the source region of the 1896 Sanriku earthquake.

3. Ocean Bottom Deformation due to the 1896 Sanriku Earthquake

Tanioka and Satake [1996b] estimated the fault parameters (length, 210 km; width, 50 km; strike, 190°; dip angle, 20°; rake, 90°) of the 1896 Sanriku tsunami earthquake by using tsunami waveforms. The location of the fault is shown in Figure 3. We use the same parameters except the dip angle. *Umino et al.* [1995] relocated micro-earthquakes off the Tohoku region using the sP depth phase and indicated that the dip angle of the plate interface near the source region is less than 10°. Therefore, we use a dip angle of 10° instead of 20°. The elastic ocean bottom deformation due to the 1896 earthquake is computed from those fault parameters using the equations of *Okada* [1985]. The sum of this elastic deformation and the additional uplift caused by the above models (A, B, or C) is used as the ocean bottom deformation due to the earthquake.

4. Tsunami Computation

In order to compute tsunami propagation, initial water surface deformation must be estimated. In general, the water surface deformation due to faulting of a large earthquake is assumed to be the same as the ocean bottom deformation, because the wavelength of the ocean bottom deformation is much larger than the ocean depth. However, this assumption cannot be applied in this study, because the width of the additional deformation (Figure 2) is about 7 km, which is similar to the ocean depth near the source region. Kajiura [1963] showed that the water surface deformation, $\eta(x,y)$, due to the ocean bottom deformation, $H_B(x_0,y_0)$, is expressed by the following equation:

$$\eta(x,y) = \iint_S H_B(x_0,y_0) R dx_0 dy_0 \qquad (1)$$

where

$$R = (1/\pi)\sum_{n=0}^{\infty}(-1)^n(2n+1)\left\{(2n+1)^2 + (x-x_0)^2 + (y-y_0)^2\right\}^{-3/2} \qquad (2)$$

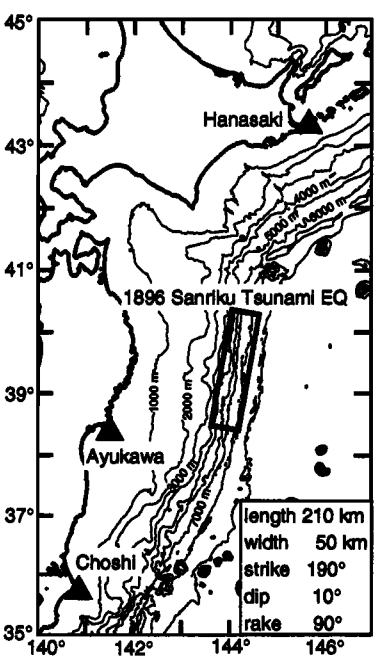

Figure 3. The tsunami computation area and the fault parameters of the 1896 Sanriku tsunami earthquake. Rectangle shows the location of the fault. Stars show the location of tide gauges.

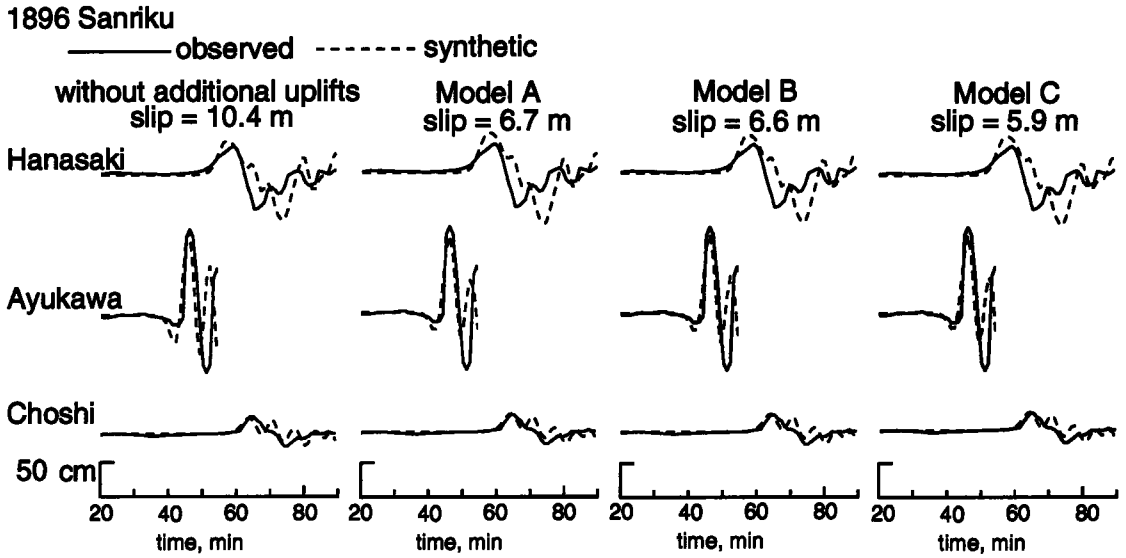

Figure 4. Comparison of observed and computed tsunami waveforms from four models, the vertical deformation without additional uplifts (left), and that with the additional uplifts of Model A, B, and C.

In the above equations, physical variables are written in non-dimensional form as follows: $x=x'/d$, $y=y'/d$, and $\eta=\eta'/d$ where a prime indicates a dimensional variable and d is the water depth. We numerically compute the water surface deformation, $\eta(x,y)$, using the above equations and use as the initial condition of the tsunami computation.

The tsunami propagation is computed by numerically solving the linear Boussinesq equation in a spherical coordinate system. The method of the numerical computation is the same as that used by Tanioka [2000]. The computational area is shown in Figure 3. The grid spacing is 20 sec of arc (about 600 m).

5. Tsunami Waveforms and Estimated Slips

The observed tsunami waveforms at three tide gauges, Hanasaki, Ayukawa, and Choshi, are used for this analysis (Figure 4). However, considering the poor accuracy of the tide gauge clocks in 1896 [*Tanioka and Satake*, 1996b], we use the waveforms without absolute timing. We compute the tsunami waveforms at the three tide gauges using three ocean bottom deformation models; one is the elastic deformation only, the other three are the elastic deformation with the additional uplift caused by Models A, B, and C as detailed above. Comparisons of the observed and computed tsunami waveforms are shown in Figure 4. The first arrivals for all stations are adjusted to match. Slip on the fault for each model is estimated by comparing the amplitudes of the first pulse of the observed and computed tsunami waveforms.

The estimated slips are 10.4 m for the model using the elastic deformation only, and 6.7 m, 6.6 m, and 5.9 m for the elastic deformations with the additional uplift caused by Models A, B and C, respectively. The estimated slip for the model using the elastic deformation only is larger than that estimated by *Tanioka and Satake* [1996b]. The main reason is that the dip angle, 10°, for the fault model in this study is smaller than that, 20°, used by *Tanioka and Satake* [1996b]. The estimated slips from the two additional uplift models, Models A and B, are almost the same, but those are slightly larger than that from Model C. These results indicate that the estimated slip due to the 1896 Sanriku earthquake becomes 5.9-6.7 m by adding an additional uplift; significantly less than 10.4 m from the purely elastic model. The uplift due to the sediments near the trench has therefore a large effect on the generation of the tsunami.

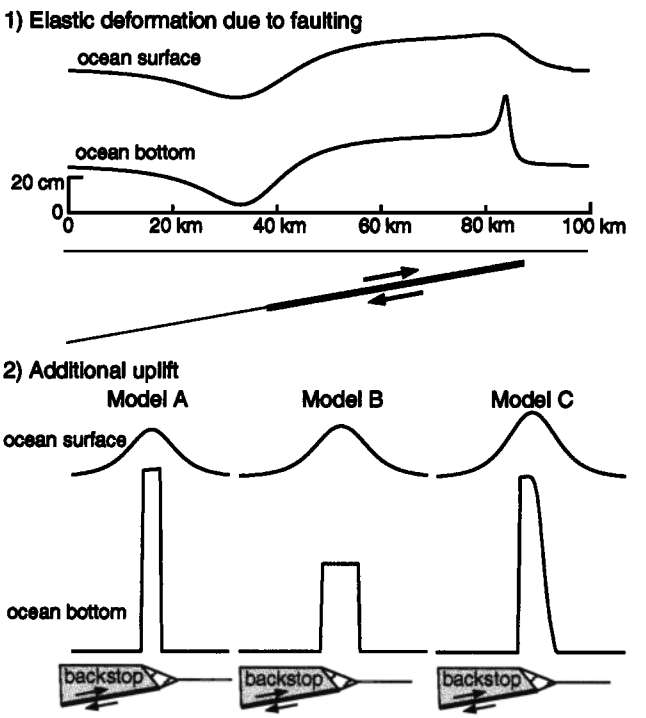

Figure 5. Comparison of ocean bottom and ocean surface deformations for (1) the elastic deformation due to faulting, and (2) the additional uplift caused by Model A, B, and C. Cross-sections of initial ocean surface deformations (top), ocean bottom deformations (middle), and the location of the fault or the sediment block (bottom) are shown for each model. The same scales are used for all cases.

Figure 5 shows the cross-section of the ocean bottom and the ocean surface deformations for the elastic deformation and three additional uplifts caused by Model A, B, and C. The cross-section was taken along a line perpendicular to the fault strike at a position of the middle of the fault. The slip on the fault is 1 m for all cases in Figure 5. The ocean surface deformation is computed from the ocean bottom deformation by applying equation (1). The ocean surface deformations for Models A, B, and C become similar although the ocean bottom deformations from the three models are quite different. Therefore, the tsunami waveforms computed from the elastic deformation with the additional uplifts caused by Models A, B, and C become similar as shown in Figure 4.

In general, the observed tsunami waveforms are equally explained by the computed tsunami waveforms from the three models. However, in detail, a small difference exists in the initial down pulse at Ayukawa. The computed down pulses from the three models with the additional uplifts are smaller and closer to the observed waveform than that from the model without the additional uplift. The additional uplifts added near the trench did not affect the subsidence located toward the coast and away from the trench (Figure 5). The initial down pulse was generated by this subsidence. Hence, the smaller slip estimated for the three models with additional uplifts generate a smaller initial down pulse than the model without additional uplift. This may indicate that the additional uplifts better explain the tsunami waveform at Ayukawa.

6. Discussion and Conclusion

The additional uplift of the sediments near the trench has a large effect on the tsunami generation. To explain the tsunami waveforms of the 1896 Sanriku tsunami earthquake recorded at the three tide gauges, the slip on the fault was reduced from 10.4 m to 5.9-6.7 m by including the additional uplift of the sediments. The observed waveforms are also well explained by the computed waveforms. The seismic moment of the 1896 Sanriku tsunami earthquake is computed to be 12-14 x 10^{20} Nm (Mw=8.0-8.1) by assuming that the rigidity around such a shallow fault is 2 x 10^{10} N/m^2.

The mechanism of tsunami earthquakes was first proposed by *Kanamori* [1972] who indicated that the large discrepancy between seismic and tsunami waves of tsunami earthquakes is caused by slow and long rupture processes. *Palayo and Weins* [1992], using seismic wave analysis, similarly concluded that tsunami earthquakes are slow thrust events in the accretionary wedge. However, it has been noticed that slow slips alone are not enough to explain anomalous excitation of tsunamis associated with some events, such as the 1896 Sanriku and 1946 Aleutian earthquakes. *Fukao* [1979] and *Okal* [1988] then proposed that an earthquake source within a shallow sedimentary layer, might excite much larger tsunamis than in solid rock, and be responsible for such anomalous tsunamis. *Satake and Tanioka* [1999], using tsunami waveform analysis, concluded that most moment release of tsunami earthquakes occurs in a narrow region near the trench and the concentrated slip is responsible for the large tsunamis. In this paper, we indicate that tsunami earthquakes are caused not only by a slow rupture process or a concentrated slip in the accretionary wedge, but also by an additional uplift of the sediments near the trench due to a large coseismic horizontal movement of the backstop. The horizontal trench-ward displacement of the backstop leads to overall folding of the accretionary prism.

Acknowledgments. We thank Drs. K. Kanjo and A. Yoshida for helpful discussions. This manuscript was greatly improved by the comments from two reviewers, Dr. E. L. Geist and Dr. K. Satake. We also thank Dr. J. M. Johnson for helpful comments to polish the manuscript and Dr. T. Yamamoto for technical supports to use the MSC/NASTRAN software.

References

Abe, K., Size of great earthquakes of 1873-1974 inferred from tsunami data, *J. Geophys. Res. 84*, 1561-1568, 1979.

Abe, K, Physical size of tsunamigenic earthquakes of the northwestern Pacific. *Phys. Earth Planet. Inter. 27*, 194-205, 1981.

Abe, K., Instrumental magnitudes of historical earthquakes, 1892-1898, *Bull. Seism. Soc. Am. 84*, 415-425, 1994.

Byrne, D. E., D. M. Davis, and L. R. Sykes, Loci and maximum size of thrust earthquakes and the mechanics of the shallow region of subduction zones, *Tectonics, 7*, 833-857, 1988.

Cardet, J.-P., K. Kobayashi, J. Aubouin, J. Boulegue, C. Deplus, J. Dubois, R. von Huene, L. Jolivet, T. Kanazawa, J. Kasahara, K. Koizumi, S. Lallemand, Y. Nakamura, G. Pautot, K. Suyehiro, S. Tani, H. Tokuyama, and T. Yamazaki, The Japan trench and its juncture with the Kuril trench: cruise results of the Kaiko project, Leg 3, *Earth and Planet. Science Lett. 83*, 267-284, 1987.

Davis, D., J. Suppe, and F. A. Dahlen, Mechanics of fold-and-thrust belts and accretionary wedges, *J. Geophys. Res. 88*, 1153-1172, 1983.

Fukao, Y., Tsunami earthquakes and subduction processes near deep-sea trenches, *J. Geophys. Res., 84*, 2303-2314, 1979.

Kajiura, K., The leading wave of a tsunami, *Bull. Earth. Res. Inst. Univ. Tokyo 41*, 535-571, 1963.

Kanamori, H., Mechanism of tsunami earthquake, *Phys. Earth Planet. Inter. 6*, 246-259, 1972.

Kobayashi, K., K. Tamaki, H. Fujimoto, M. Nakanishi, J. Oshida, D. C. P. Masalu, Y. Ogawa, H. Iino, T. Tsukioka, K. Kashihara, T. Matsumoto, T. Tanaka and T. Furuta., Results of bathymetric measurement, *Prelim. Rep. Hakuho Maru Cruise KH90-1*,10-11, 1991.

Okada, Y.. Surface deformation due to shear and tensile faults in a half-space, *Bull. Seism. Soc. Am. 75*, 1135-1154, 1985.

Okal, E. A., Seismic parameters controlling far-field tsunami amplitudes: a review, *Natural Hazards, 1*, 67-96, 1988.

Pelayo, A.M., and D.A. Wiens, Tsunami earthquakes: slow thrust-faulting events in the accretionary wedge, *J. Geophys. Res., 97*, 15321-15337, 1992.

Satake, K. and Y. Tanioka, Source of tsunami and tsunamigenic earthquakes in subduction zones, *Pure and Appl. Geophys. 154*, 467-483, 1999.

Seno, T., The 21 September, 1999 Chichi earthquake in Taiwan: implications for tsunami earthquakes, *Terr. Atmos. Ocean Sci. 11*, 701-708, 2000.

Tanioka, T. and K. Satake, Tsunami generation by horizontal displacement of ocean bottom, Geophys. Res. Lett. 23, 861-864, 1996a.

Tanioka, T. and K. Satake, Fault parameters of the 1896 Sanriku tsunami earthquake estimated from tsunami numerical modeling, *Geophys. Res. Lett. 23*, 1549-1552, 1996b.

Tanioka, T., Numerical simulation of far-field tsunami using the linear Boussinesq equation, *Pap. Meteorol. Geophys., 51*, 17-25, 2000.

Umino, N., A. Hasegawa, and T. Matsuzawa, sP depth phase at small epicentral distances and estimated subducting plate boundary, *Geophys. J. Int. 120*, 356-366, 1995.

T. Seno, Earthquake Research Institute, University of Tokyo, Tokyo 113-0032, Japan. (e-mail: seno@eri.u-tokyo.ac.jp)

Y. Tanioka, Seismology and Volcanology Research Department, Meteorological Research Institute, 1-1 Nagamine, Tsukuba 305-0052, Japan. (e-mail: ytanioka@mri-jma.go.jp)

(Received March 9, 2001; revised June 1, 2001;
accepted June 28, 2001.)